Catalysis Letters 65 (2000) 91–98

Studies on the redox behaviour of $La_{1.867}Th_{0.100}CuO_4$ and its catalytic performance for NO decomposition

L.Z. Gao * and C.T. Au **

Chemistry Department and Center for Surface Analysis and Research, Hong Kong Baptist University, Kowloon Tong, Hong Kong, PR China
E-mail: pctau@hkbu.edu.hk

Received 19 September 1999; accepted 14 January 2000

$La_{1.867}Th_{0.100}CuO_4$ was prepared by means of the citric acid complexing method. The reduction–oxidation (redox) properties of this composite oxide have been investigated by using the XRD, TGA, EPR, TPD, and SEM methods. The fresh (non-reduced) $La_{1.867}Th_{0.100}CuO_4$ catalyst is single phase with tetragonal K_2NiF_4-type structure. There were three reduction steps observed over $La_{1.867}Th_{0.100}CuO_4$ in the temperature ranges of 25–100, 100–300, and 300–500 °C, respectively. After reduction at 300 °C, the material still retained its original single phase but there were oxygen vacancies generated in the lattice. After reduction at 500 °C, it decomposed to a mixture of oxides. In the course of reduction, trapped electrons were generated. During the oxidation of the reduced sample, O_2^- was detected. Apparently, oxygen vacancies are able to stabilise O_2^- on the surface of the catalyst. NO adsorption on both the fresh and reduced $La_{1.867}Th_{0.100}CuO_4$ samples generated NO radicals and O_2^- species. On a $La_{1.867}Th_{0.100}CuO_4$ sample reduced at 300 °C, $[O_2NO_2]^{2-}$ was generated in NO adsorption and decomposed to N_2 and O^{2-} at ca. 730 °C. After reduction, the O^{2-} inside the $La_{1.867}Th_{0.100}CuO_4$ lattice became more mobile and participated in the decomposition of $[O_2NO_2]^{2-}$. The fresh (non-reduced) $La_{1.867}Th_{0.100}CuO_4$ sample with cation defects in its lattice shows higher NO decomposition activity than the fresh La_2CuO_4 sample in which there are no cation defects. The 300 °C-reduced $La_{1.867}Th_{0.100}CuO_4$ with cation defects and oxygen vacancies is more active than the fresh one for NO decomposition. The redox action between Cu^+ and Cu^{2+} is an essential process for NO decomposition.

Keywords: $La_{1.867}Th_{0.100}CuO_4$, redox behaviour, NO decomposition

1. Introduction

Perovskite type (ABO_3) mixed oxides are known to be active catalysts for NO_x reduction and ammonia oxidation [1,2]. They are thermally stable (up to 1000 °C) and can accommodate lattice defects such as oxygen vacancies, A-site deficiencies, and B ions of variable oxidation states. The perovskite-like A_2BO_4 mixed oxides of K_2NiF_4 structure are thermally more stable than ABO_3 and have been described as novel catalysts for ammonia oxidation and NO_x elimination [3–5]. In general, in ABO_3 and A_2BO_4, A is a rare earth element and B is a transition metal; the oxidation state of B is 2+ and 3+, respectively, in the two compounds. Besides noble metals such as Pt, Pd, Ru, and Rh, copper is also a common component in $DeNO_x$ catalysts. Unlike $LaMnO_3$, $LaFeO_3$, $LaCoO_3$, and $LaNiO_3$, the compound $LaCuO_3$ is unstable because it is difficult to keep a high concentration of Cu^{3+} in the bulk of $LaCuO_3$. In contrast, La_2CuO_4 is very stable [5]. The working oxidation state of copper for the $DeNO_x$ reaction is unclear. For the Cu-ZSM-5 catalysts, Cu^+ was thought to be an active center [6,7]. London et al. suggested that NO decomposition is associated with a redox between Cu^+ and Cu^0 [8]. Mizuno et al. reported that Cu^{2+} is an active center for NO decomposition [9]. The role played by oxygen in the NO decomposition reaction is a topic of controversy [10]. Most of the $DeNO_x$ catalysts are SCR (selective catalytic reduction) catalysts. The SCR process needs additional reductant(s) such as hydrocarbons, CO, H_2 or NH_3; this leads to the production of secondary pollutants such as oxygenated hydrocarbons, CO, CO_2, N_2O or cyanate and isocyanate compounds [10]. The direct catalytic decomposition of NO to N_2 and O_2 is highly desirable because no additional reactant is needed for the reaction. However, up to now, no suitable material has been obtained to catalyse the reaction under actual exhaust conditions [10–12]. The influence of cation defects on the catalytic activity of NO decomposition was rarely reported. The radius of Th^{4+} (0.94 Å) is smaller than that of La^{3+} (1.23 Å). The substitution of Th^{4+} for La^{3+} is possible. Based on such an understanding, we synthesised $La_{1.867}Th_{0.100}CuO_4$ as a catalyst for NO decomposition. According to the $La_{1.867}Th_{0.100}CuO_4$ stoichiometry, 1.65% of the A-site ions are defects. The activity of the catalyst for NO decomposition has been investigated as related to the intrinsic defect properties of the material.

2. Experimental

2.1. Catalyst preparation

The catalyst was prepared by the citric acid complexing method: lanthanum, thorium, and copper nitrates in a

* Present address: Chengdu Institute of Organic Chemistry, Chinese Academy of Sciences, Chengdu 610041, PR China.
** To whom correspondence should be addressed.

© J.C. Baltzer AG, Science Publishers

desired molar ratio were dissolved in a citric solution at 80 °C with constant stirring until a viscous gel was formed. The gel was decomposed abruptly to very fine powder (ca. 10 nm) at around 300 °C. The furnace temperature was then raised (20 °C min^{-1}) to 500 °C and the catalyst was heated at this temperature in air for 5 h. After being pressed and ground, the catalyst was calcined at 950 °C for 12 h.

2.2. Characterisation

The metal-ion composition of the catalyst was determined by titration against standardised solution of EDTA. The oxidation state of copper in the catalyst was measured by means of the iodometry method [13,14]. Together with the known contents of La^{3+} and Th^{4+}, the data were used to estimate the non-stoichiometric amount of oxygen in the sample.

XRD measurements were carried out on a Rigaku D-Max Rotaflex instrument with Cu Kα radiation and Ni filter. BET specific areas were measured on a Nova 1200 instrument. The samples were first treated in a vacuum for 2 h at 400 °C before BET measurements.

H_2-TGA was performed on a Rigaku thermoanalyser. For each measure, 40 mg of fresh (non-reduced) sample was used. A mixture of 10% H_2–90% He (flow rate 20 ml min^{-1}) was passed through the sample. The temperature range studied was from 20 to 500 °C and the heating rate was 10 °C min^{-1}.

EPR spectra were recorded at −196 °C with a Jeol spectrometer operating in the X-band and calibrated with DPPH ($g = 2.004$). The sample (0.1 g) was placed in a self-made quartz cell in which the sample could be treated under different atmospheres at various temperatures. Before performing the EPR studies over fresh or 300 °C-reduced $La_{1.867}Th_{0.100}CuO_4$, we He-purged (flow rate 20 ml min^{-1}) the sample at 800 °C for 1 h and then cooled it down to 25 °C in He. For NO adsorption, NO (3000 ppm with He being the carrier gas, flow rate 20 ml min^{-1}) was introduced into the quartz cell at a desired temperature for 1 h. For the redox studies of $La_{1.867}Th_{0.100}CuO_4$, the sample was reduced in H_2 (H_2/He = 1/9, flow rate 20 ml min^{-1}) at 100, 300, and 500 °C, respectively. The 500 °C-reduced sample was then exposed to O_2 (flow rate 20 ml min^{-1}) at a desired temperature for 1 h. After NO or O_2 exposure, the sample was He-purged (flow rate 20 ml min^{-1}) and then quenched in liquid nitrogen. For each EPR measurement of NO adsorption, a new sample was used and the procedures were repeated.

For TPD studies, the sample (0.2 g) was placed in the middle of a quartz reactor (i.d. 4 mm). The outlet gases were analysed on line by mass spectrometry (MS, HP G 1800A). The heating rate was 8 °C min^{-1} and the temperature range was from 20 to 800 °C. The O_2-TPD experiment was performed according to the following procedures: The sample was first heated in O_2 at 300 °C for 1 h and then cooled to room temperature in O_2. After being He-purged at room temperature for 1 h, the sample was heated to 800 °C in a helium flow (20 ml min^{-1}). The NO-TPD experiment was performed according to the following procedures: The sample was first calcined *in situ* at 800 °C for 1 h under a flow of He (20 ml min^{-1}) and then cooled to room temperature. The sample was kept in a flow of NO/He (v/v = 1/100, flow rate 20 ml min^{-1}) for 1 h at 300 °C and then cooled to room temperature. After being He-purged at room temperature for 1 h, the sample was heated to 800 °C in helium (20 ml min^{-1}).

SEM pictures were obtained on a Jeol JXA-840 scanning electron microscope at 15 kV with an amplitude of 10000.

2.3. Catalytic activity measurements

Catalytic activity evaluation was carried out with 0.3 g of sample packed in a quartz microreactor. Prior to the test, the sample was treated at 650 °C under a He flow to eliminate water and carbonates. The decomposition of NO was performed between 200 and 800 °C (heating rate 2 °C min^{-1}). The reaction feed was 3000 ppm NO in He and the total GHSV was 7500 h^{-1}. Catalytic activity was measured 0.5 h after performance stabilisation. The effluent gases (N_2, NO, and N_2O) were analysed by gas chromatography and mass spectrometry. Before evaluating the catalytic activity of the reduced sample, we carried out the CD_3I-TPD procedure to eliminate surface hydrogen. After three cycles of CD_3I-TPD treatments, we observed no more CD_3H. It is an indication that most of the surface hydrogen has been eliminated.

3. Results and discussion

3.1. Redox behaviours of catalyst

Based on the data obtained according to the titration methods, the composition of $La_{1.867}Th_{0.100}CuO_4$ is actually $La_{1.867}Th_{0.100}CuO_{4.005}$ whereas that of La_2CuO_4 is $La_2CuO_{4.008}$ (table 1). The radius of Th^{4+} (0.94 Å) is smaller than that of La^{3+} (1.23 Å), the substitution of Th^{4+} for La^{3+} in the lattice is possible. Due to the substitution of Th^{4+} for La^{3+}, the concentration of Cu^{3+} in $La_{1.867}Th_{0.100}CuO_{4.005}$ is lower than that in $La_2CuO_{4.008}$. One can envision that besides the cation defects, there was an excess amount of oxygen in $La_{1.867}Th_{0.100}CuO_{4.005}$ ($La_{1.867}Th_{0.100}\phi_{0.033}CuO_{4.005}$, ϕ: cation defect).

The XRD results of fresh and the 100 °C-, 300 °C-, and 500 °C-reduced $La_{1.867}Th_{0.100}CuO_{4.005}$ samples are listed

Table 1
Cu^{3+} concentrations, surface areas, and compositions of La_2CuO_4 and $La_{1.867}Th_{0.100}CuO_4$.

Sample	Cu^{3+}/Cu (%)	Surface (m^2/g)	Composition
La_2CuO_4	1.5	2.8	$La_2CuO_{4.008}$
$La_{1.867}Th_{0.100}CuO_4$	1.0	3.5	$La_{1.867}Th_{0.100}CuO_{4.005}$

Table 2
Compositions of $La_{1.867}Th_{0.100}CuO_{4.005}$ with various treatments.

Sample	Composition[a]
$La_{1.867}Th_{0.100}CuO_{4.005}$ reduced at	
100 °C	T
300 °C	T
500 °C	T, $LaCuO_2$, La_2O_3, CuO, Cu (w)
500 °C-reduced $La_{1.867}Th_{0.100}CuO_{4.005}$ oxidised at	
⩽300 °C	T, La_2O_3, $LaCuO_2$, CuO, Cu_2O (w)
400–500 °C	T, La_2O_3, $LaCuO_2$ (w), CuO
600–700 °C	T, La_2O_3 (w), $LaCuO_2$ (vw)
800 °C	T

[a] T: tetragonal K_2NiF_4-type structure, (w): weak, (vw): very weak.

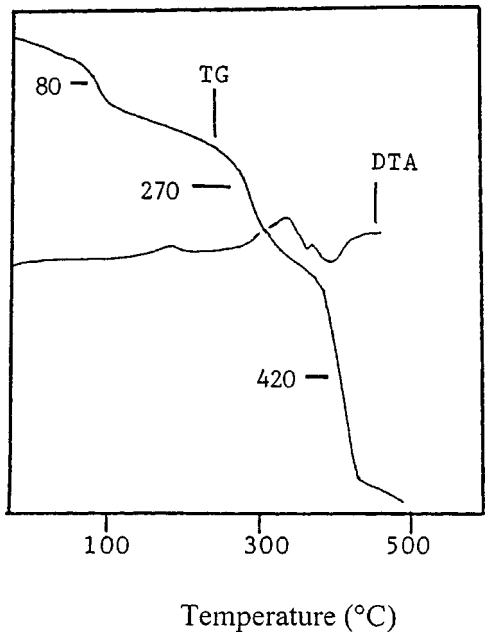

Figure 1. TGA curves of $La_{1.867}Th_{0.100}CuO_4$.

in table 2. Fresh $La_{1.867}Th_{0.100}CuO_{4.005}$ is of tetragonal K_2NiF_4-type structure. When it was reduced at 100 and 300 °C, respectively, it still retained such a structure. When it was reduced at 500 °C, it partially decomposed to $LaCuO_2$, La_2O_3, CuO, and Cu.

Figure 1 shows the TGA profiles of $La_{1.867}Th_{0.100}CuO_{4.005}$. We observed reduction steps at ca. 80, 270, and 420 °C. According to the weight losses, the composition of the sample was deduced to be $La_{1.867}Th_{0.100}CuO_{3.996}$, $La_{1.867}Th_{0.100}CuO_{3.977}$, and $La_{1.867}Th_{0.100}CuO_{3.942}$ after the first, second, and third reduction step, respectively. Based on the results of XRD and TGA analyses, we suggest that $La_{1.867}Th_{0.100}CuO_{4-\delta}$ (δ: nonstoichiometric oxygen) decomposed thoroughly when $\delta \geqslant 0.058$. In $La_{1.867}Th_{0.100}CuO_{3.996}$, almost all the copper ions were Cu^{2+}; in $La_{1.867}Th_{0.100}CuO_{3.977}$, there were 4.7% Cu^+ and 95.3% Cu^{2+}. We deduce that (i) during the first reduction step, Cu^{3+} was reduced to Cu^{2+}; (ii) during the second reduction step, Cu^{2+} was reduced to Cu^+; and (iii) during the third reduction step, the K_2NiF_4-type structure collapsed due to the deep reduction of Cu^+ and the generation of metallic copper.

Figure 2 shows the SEM pictures of the fresh and 100 °C-, 300 °C-, and 500 °C-reduced $La_{1.867}Th_{0.100}CuO_{4.005}$ samples. One can observe that after reduction, the catalyst particles were smaller in size and distributed more evenly. At a reduction temperature of 500 °C, the particles clustered together.

The EPR spectra of $La_{1.867}Th_{0.100}CuO_{4.005}$ obtained before and after reduction and oxidation are shown in figure 3. The spectrum of the fresh $La_{1.867}Th_{0.100}CuO_{4.005}$ sample exhibits intensive EPR signals with $g = 2.231$, 2.130, and 2.059 (figure 3(a)); these are typical EPR features of cupric ions [6]. The EPR line is rather broad, possibly due to the high concentration of Cu^{2+}. When the sample was reduced at 100 °C, the spectrum intensity decreased drastically, and a signal with $g = 2.007$ appeared (figure 3(b)). The 2.007 signal is attributable to electrons trapped at oxygen vacancies [15]. According to the H_2-TGA results, after being reduced at 100 °C, the catalyst became $La_{1.867}Th_{0.100}CuO_{3.996}$ and there were oxygen vacancies in the bulk. The reduction would result in Cu^{3+} being converted to Cu^{2+}. After reduction at 300 °C, the signal of trapped electrons intensified (figure 3(c)). The H_2-TGA result demonstrated that at this stage, more oxygen vacancies were generated and the sample composition was $La_{1.867}Th_{0.100}CuO_{3.977}$. The reduction would result in Cu^{2+} being converted to Cu^+. Hence, the reduction process can be described as:

at 100 °C

$$H_2 \rightarrow 2H^+ + 2e \quad (1)$$

$$Cu^{3+} + e \rightarrow Cu^{2+} \quad (2)$$

$$La_{1.867}Th_{0.100}Cu^{3+}Cu^{2+}O_{4.005} \rightarrow La_{1.867}Th_{0.100}CuO_{3.996} + V_o^{\cdot\cdot} \quad (3)$$

$$e + V_o^{\cdot\cdot} \rightarrow V_e^{\cdot} \quad (4)$$

at 300 °C

$$Cu^{2+} + e \rightarrow Cu^{+} \quad (5)$$

$$La_{1.867}Th_{0.100}Cu^{2+}O_{3.996} \rightarrow La_{1.867}Th_{0.100}Cu^{2+}Cu^{+}O_{3.977} + V_o^{\cdot\cdot} \quad (6)$$

($V_o^{\cdot\cdot}$ oxygen vacancy, $V_e^{\cdot}$ trapped electron).

When the sample was reduced at 500 °C, a signal with $g = 2.069$ appeared while the signal of trapped electrons weakened (figure 3(d)). XRD and H_2-TGA studies revealed that at this stage, the sample had partially decomposed to $LaCuO_2$, La_2O_3, CuO, and Cu. The signal with $g = 2.069$ represents a kind of cupric ion in a new coordination [16]. In other words, there was the generation of a new cupric surface complex. We speculate that the CuO and $LaCuO_2$ phases may be responsible for this new signal. The disappearance of the signal of

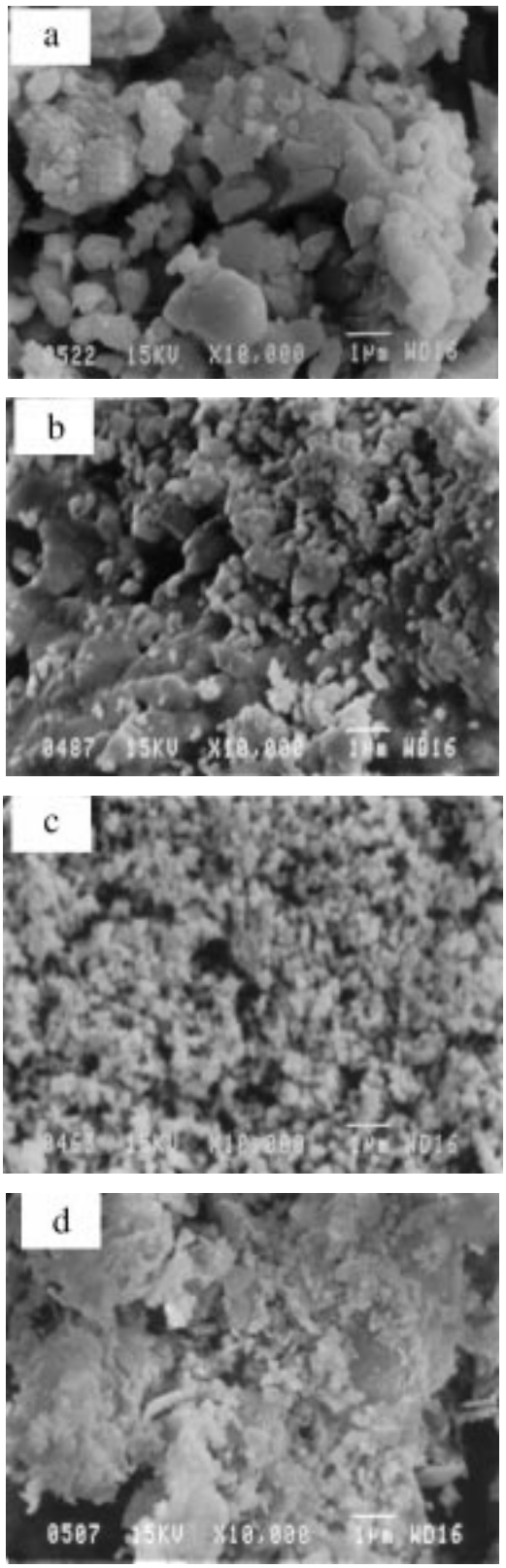

Figure 2. SEM pictures of (a) fresh, (b) 100 °C-reduced, (c) 300 °C-reduced, and (d) 500 °C-reduced $La_{1.867}Th_{0.100}CuO_4$.

trapped electrons could be due to the demolition of oxygen vacancies due to the collapse of the K_2NiF_4-type structure.

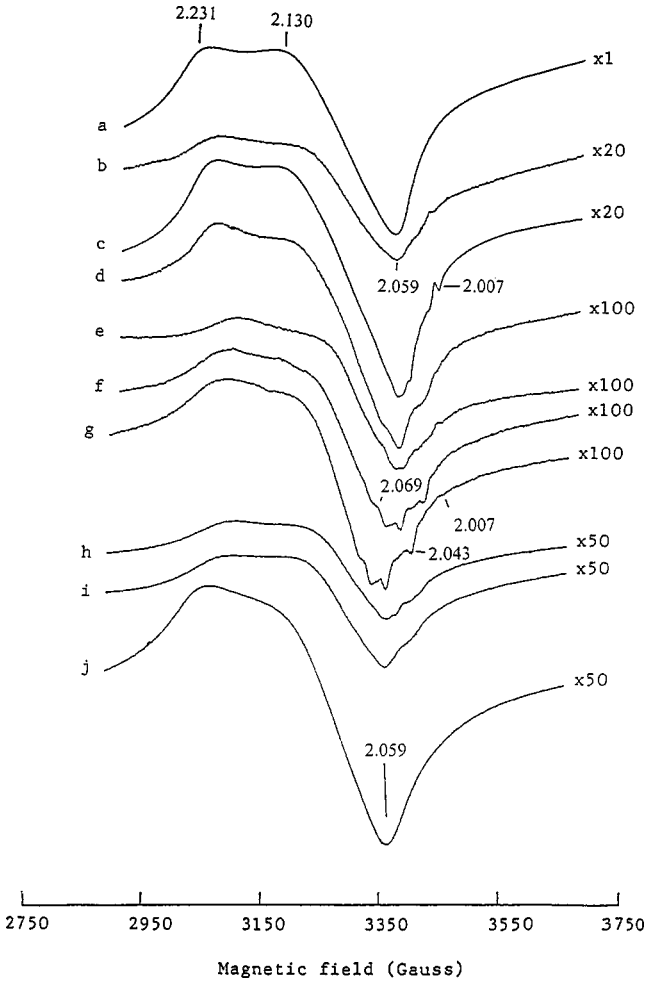

Figure 3. EPR spectra of (a) fresh, (b) 100 °C-reduced, (c) 300 °C-reduced, and (d) 500 °C-reduced $La_{1.867}Th_{0.100}CuO_4$; and those obtained after the 500 °C-reduced sample was being oxidised at (e) 300, (f) 400, (g) 500, (h) 600, (i) 700, and (j) 800 °C, respectively.

The XRD results obtained during the oxidation of the 500 °C-reduced sample are also listed in table 2. There was the tetragonal K_2NiF_4-type phase as well as the La_2O_3, CuO, $LaCuO_2$, and Cu_2O phases after oxidation at temperatures below 300 °C. Between 400 and 500 °C, there were the tetragonal K_2NiF_4-type phase as well as the La_2O_3, $LaCuO_2$, and CuO phases. Between 600 and 700 °C, there were a little amount of La_2O_3 and a trace of $LaCuO_2$ but a large amount of the K_2NiF_4-type phase. At 800 °C, the sample recovered to the former single K_2NiF_4-type structure. Figure 3 (e)–(j) shows the EPR spectra of a reduced sample being oxidized under an oxygen flow at temperatures between 300 and 800 °C. There was no significant change when the oxidation temperature was below 300 °C (figure 3(e)). When the reduced sample was oxidised at 400 and 500 °C, signals with $g = 2.007$, 2.043, and 2.069 could be observed (figure 3 (f) and (g)). The signals with g values of ca. 2.007 and 2.043 are attributable to O_2^- ions at oxygen vacancies [17–19]. It has been suggested that surface O_2^- species could be formed during thermal treatment *in vacuo* [19]; these oxygen species could enter the oxygen

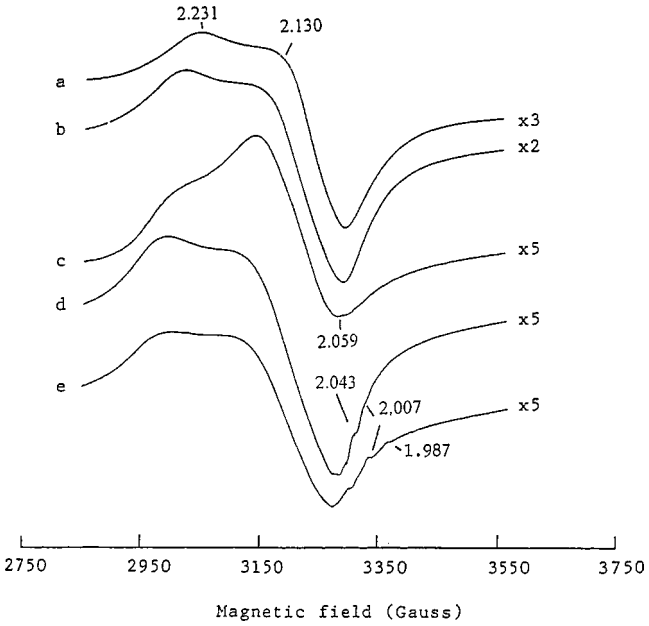

Figure 4. EPR spectra of NO adsorption on fresh $La_{1.867}Th_{0.100}CuO_4$ at (a) 200, (b) 300, (c) 400, (d) 500, and (e) 600 °C, respectively.

vacancies and participate in the transfer of electrons [18]. As mentioned before, the signal with $g = 2.069$ could be due to a new kind of cupric ions at a different coordination environment. At 600 and 700 °C, these signals weakened in intensity (figure 3 (h) and (i)). The XRD results showed that at these stages, there was a large amount of K_2NiF_4-type phase. At 800 °C, the EPR spectra (figure 3(j)) recovered to a feature similar to that of a fresh $La_{1.867}Th_{0.100}CuO_{4.005}$ sample, indicating that the mixtures had been converted back to the single K_2NiF_4-type structure.

3.2. The interaction of NO with fresh $La_{1.867}Th_{0.100}CuO_{4.005}$

Figure 4 shows the EPR spectra of NO adsorption on fresh $La_{1.867}Th_{0.100}CuO_{4.005}$ at temperatures ranging from 200 to 600 °C. We observed no changes in spectrum features below 400 °C (figure 4 (a)–(c)), indicating that there was little interaction between NO and the fresh catalyst. At 500 °C, there were signals with $g = 2.007$ and 2.043 (figure 4(d)), attributable to O_2^- at oxygen vacancies [17]. At 600 °C, there was a signal with $g = 1.987$, which can be attributed to NO radicals of low mobility [17]. NO adsorption can generate NO^+, NO^-, and $(NO_2)^-$ species [10]. NO^+ is EPR silent. In general, NO^- has been considered as a reaction intermediate for NO decomposition because the bond order of NO^- is 2.0 [20,21].

3.3. NO interaction with $La_{1.867}Th_{0.100}CuO_{4.005}$ pre-reduced at 300 °C

Figure 5 shows the EPR spectra of NO adsorption on reduced (at 300 °C) $La_{1.867}Th_{0.100}CuO_{4.005}$ from 100 to 700 °C. We observed that after NO adsorption at 100, 200,

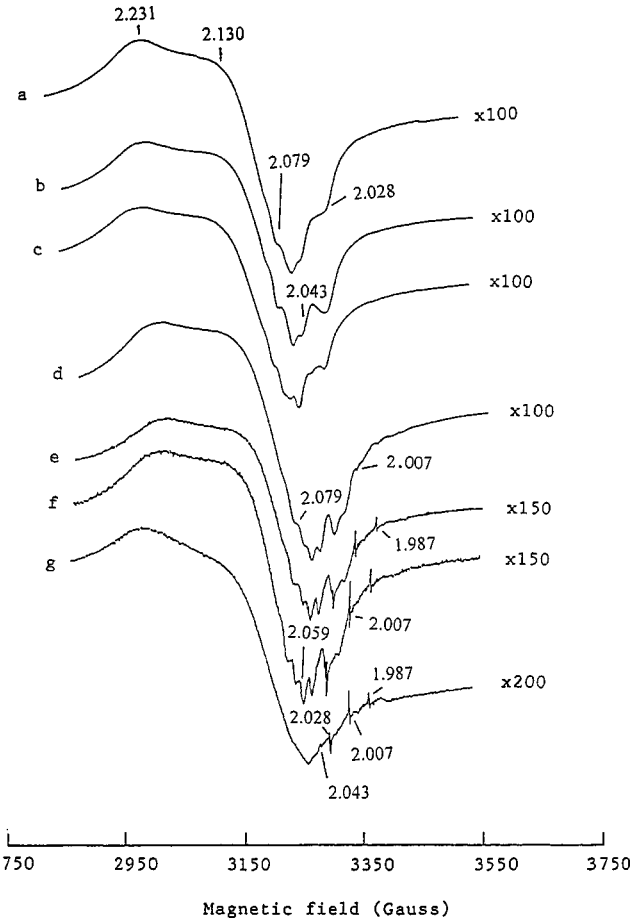

Figure 5. EPR spectra of NO adsorption on a 300 °C-reduced $La_{1.867}Th_{0.100}CuO_4$ sample at (a) 100, (b) 200, (c) 300, (d) 400, (e) 500, (f) 600, and (g) 700 °C, respectively.

and 300 °C, there were signals with $g = 2.079$, 2.043, and 2.028 (figure 5 (a)–(c)). The signal with $g = 2.079$ can be assigned to Cu^{2+} [22]. In other words, NO had oxidised Cu^+ to Cu^{2+}. We deduce that there could be the formation of cupric nitrate. Yasuda et al. [23] reported that in La_2CuO_4-based mixed oxides, NO oxidised Cu^{2+} to Cu^{3+}. Munakata et al. [24] reported that in $LaBaSrCu_2O_6$, NO adsorption would result in the formation of nitrates. The signal with $g = 2.028$ can be assigned to the interaction of NO with O_2^- at oxygen vacancies, probably in the form of $[O_2NO_2]^{2-}$ [17]. Again, the signal with $g = 2.043$ is due to O_2^- at oxygen vacancies.

When the NO adsorption temperature was 400 °C, there were signals with $g = 2.007$, 2.028, 2.043, and 2.079 (figure 5(d)). The signals at 2.007 and 2.043, 2.028, and 2.079 are due to O_2^- at oxygen vacancies, $[O_2NO_2]^{2-}$, and cupric nitrate, respectively. When the adsorption temperature was 500 or 600 °C, besides the signals observed in figure 5(d), there was a signal with $g = 1.987$ (figure 5 (e) and (f)). The signal with $g = 1.987$ is due to NO radicals [17]. At an adsorption temperature of 700 °C, there were obvious changes in EPR feature (figure 5(g)). The signals at 1.987, 2.007, 2.028, and 2.043 still existed, whereas the signal of cupric nitrate vanished. Lin et al. reported that

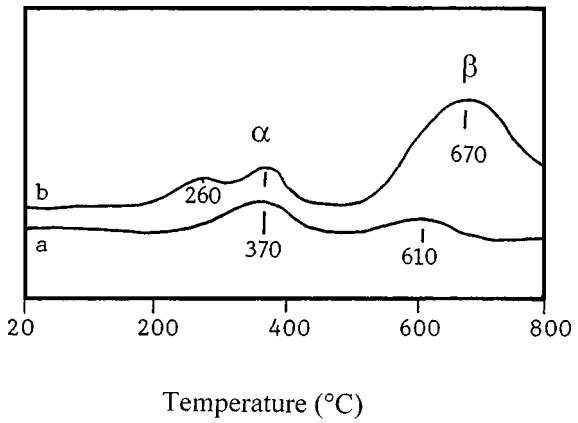

Figure 6. O_2-TPD profiles obtained after O_2 adsorption at 300 °C over (a) a fresh and (b) a 300 °C-reduced $La_{1.867}Th_{0.100}CuO_4$.

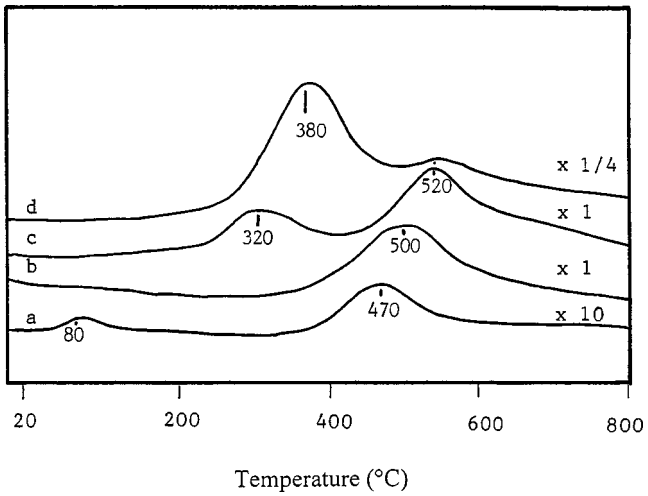

Figure 7. MS spectra obtained in NO-TPD study over a fresh $La_{1.867}Th_{0.100}CuO_4$ sample: (a) NO_2, (b) N_2, (c) N_2O, and (d) NO.

nitrate ion was the predominant species at temperatures below 267 °C, and its concentration decays at elevated temperatures (>547 °C) [25].

3.4. TPD studies

Figure 6 shows the O_2-TPD curves obtained over the fresh and 300 °C-reduced $La_{1.867}Th_{0.100}CuO_{4.005}$ samples. There are two O_2-desorption peaks centered at 370 and 610 °C over the fresh sample and three O_2-desorption peaks at ca. 260, 370, and 670 °C over the reduced one. In general, there are two kinds of O_2 desorption observed on perovskite-type oxides [26]. One is the oxygen (α) at oxygen vacancies and the other is lattice oxygen (β) associated with the redox of B ions. There are two α peaks in figure 6(b), implying that compared to the fresh sample, there were more oxygen vacancies in the reduced sample. The β peak (at 670 °C) in figure 6(b) was bigger than that (at 610 °C) in figure 6(a), indicating that the lattice oxygen in the reduced sample is more mobile than that in the fresh one.

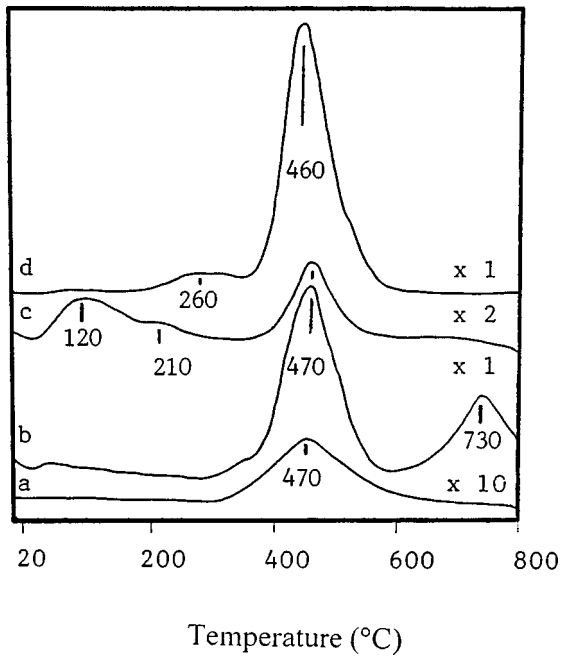

Figure 8. MS spectra obtained in NO-TPD study at 300 °C over a 300 °C-reduced $La_{1.867}Th_{0.100}CuO_4$ sample: (a) O_2, (b) N_2, (c) N_2O, and (d) NO.

Figures 7 and 8 are the MS spectra of NO-TPD obtained over the fresh and 300 °C-reduced $La_{1.867}Th_{0.100}CuO_{4.005}$ samples, respectively. NO adsorption on the fresh sample produced NO_2 (at ca. 80 and 470 °C) (figure 7(a)), N_2 (at ca. 500 °C) (figure 7(b)), N_2O (at ca. 320 and 520 °C) (figure 7(c)), and NO (at ca. 380 and 570 °C) (figure 8(d)). We did not observe O_2 desorption during the TPD process on a fresh sample. Apparently, there were two different processes for N_2O generation and only one for N_2 production on the fresh sample. As for NO-TPD studies on a reduced sample, we observed O_2 desorption at ca. 470 °C (figure 8(a)), N_2 desorption at ca. 470 and 730 °C (figure 8(b)), N_2O desorption at ca. 120, 210, and 470 °C (figure 8(c)), and NO desorption at ca. 260 and 460 °C (figure 8(d)). Around 470 °C, N_2, O_2, NO, and N_2O were produced; whereas, around 730 °C, only N_2 was detected. Apparently, there were two different processes for N_2 generation on the reduced sample, one occurred at ca. 470 °C and that other at ca. 730 °C.

3.5. Catalytic activity and redox action

The catalytic activities of NO decomposition at 500 °C over the La_2CuO_4 catalyst and the fresh, and 100 °C-, 300 °C-, and 500 °C-reduced $La_{1.867}Th_{0.100}CuO_{4.005}$ samples are listed in table 3. The main products were N_2 and N_2O. The activity of NO decomposition to N_2 decreases in the order of: 300 °C-reduced > 100 °C-reduced > fresh > 500 °C-reduced $La_{1.867}Th_{0.100}CuO_{4.005}$ > La_2CuO_4. The results indicated that the sample of single phase K_2NiF_4-type structure possessing oxygen vacancies and cation defects performed the best. After reduction at 300 °C, there was the generation of Cu^+ and Cu^{2+}. Reduction at 500 °C

Table 3
Catalytic activities at 500 °C of La_2CuO_4 (fresh) and $La_{1.867}Th_{0.100}CuO_{4.005}$ (fresh, 100 °C-, 300 °C-, and 500 °C-reduced) catalysts.

	Catalyst				
	La_2CuO_4	$La_{1.867}Th_{0.100}CuO_{4.005}$			
	fresh[a]	fresh[a]	100[b]	300[b]	500[b]
NO conversion N_2 (%)	20	26	40	65	25
NO conversion N_2O (%)	5	21	12	7	7

[a] Fresh: non-reduced.
[b] Reduction temperature (°C).

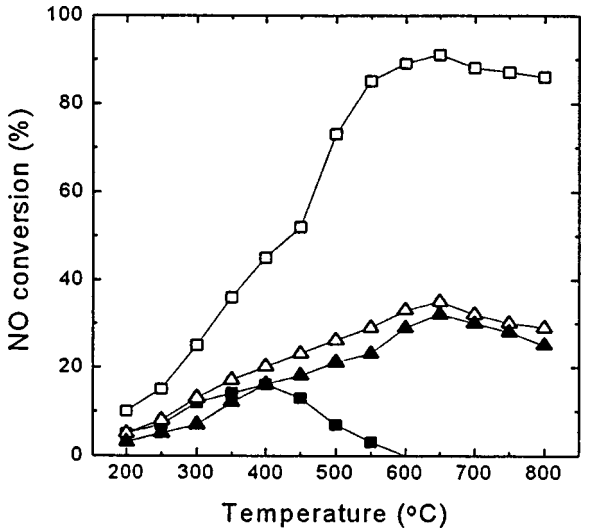

Figure 9. NO conversion to N_2 (△, □) and N_2O (▲, ■) versus reaction temperature over fresh (△, ▲) and 300 °C-reduced (□, ■) $La_{1.867}Th_{0.100}CuO_4$.

would result in Cu^0 formation. We suggest that the decomposition process of NO can be related to a redox action between Cu^+ and Cu^{2+} in the K_2NiF_4-type lattice. Figure 2 shows that the particles of the 300 °C-reduced $La_{1.867}Th_{0.100}CuO_{4.005}$ sample were the smallest; therefore, we propose that a small particle size would be beneficial to NO decomposition.

Figure 9 shows the conversion of NO to N_2 and N_2O as a function of temperature (200–800 °C) over the fresh and 300 °C-reduced $La_{1.867}Th_{0.100}CuO_{4.005}$ catalysts. Within the temperature range, the performance of the reduced sample was better than that of the fresh one. At 650 °C, we obtained 91% NO conversion (to N_2) over the former and 35% NO conversion (to N_2) over the latter; N_2O was a by-product. Gervasini et al. reported the catalytic performances of NO direct decomposition over γ-Al_2O_3-supported Ru, Rh, Pd, and Pt catalysts [27]. The catalytic activities at optimum reaction temperatures are: (i) Ru/γ-Al_2O_3, 10.0% NO conversion to N_2 at 700 °C; (ii) Rh/γ-Al_2O_3, 31.8% NO conversion to N_2 at 600 °C; (iii) Pd/γ-Al_2O_3, 81.6% NO conversion to N_2 at 800 °C; (iv) Pt/γ-Al_2O_3, 82.6% NO conversion to N_2 at 800 °C. Iwamoto et al. reported 80% NO conversion to N_2 at an optimum reaction temperature of 527 °C over a Cu-MFI-143 catalyst [28]. We found that the catalytic activity of NO decomposition to N_2 over the 300 °C-reduced $La_{1.867}Th_{0.1}CuO_{4.005}$ sample is (i) higher than over the γ-Al_2O_3-supported noble metal catalysts and (ii) lower than over Cu-MFI-143 below 550 °C but higher above 550 °C.

The EPR results demonstrated that both NO radicals and O_2^- were generated in NO adsorption on the fresh and reduced $La_{1.867}Th_{0.100}CuO_{4.005}$ samples. However, $[O_2NO_2]^{2-}$ was detected only on the latter (figure 5) but not on the former (figure 4). We hence deduce that the $[O_2NO_2]^{2-}$ species is responsible for the high activity of NO decomposition over the reduced catalyst. According to the TPD results of a reduced sample (figure 8), there was N_2 desorption but no N_2O and O_2 desorption around 730 °C. As shown in the O_2-TPD study (figure 6(b)), there was a large desorption of lattice oxygen around 670 °C. We deduce that the decomposition of $[O_2NO_2]^{2-}$ could contribute to the availability of lattice oxygen:

$$[O_2NO_2]^{2-} + 6e \rightarrow 4O^{2-} + (1/2)N_2 \qquad (7)$$

It has been reported that the addition of a small amount of oxygen could enhance $DeNO_x$ activity [29–31]. Valyon and Hall observed that the oxygen released was different from the oxygen introduced to a Cu-ZSM-5 sample [32]. Based on $^{18}O_2$ and $^{15}N^{18}O$ isotope studies, Valyon et al. proposed that an "extra-lattice-oxygen (ELO) species" was involved in NO decomposition [33,34]. Sachtler and coworkers suggested that ELO is in the form of Cu^{2+}–O^{2-}–Cu^{2+} [35,36]; whereas Larsen et al. suggested that ELO is in the form of $Cu^{2+}O^-$ or $Cu^{2+}O_2^-$ [37]. Iwamoto et al. reported that at high temperatures, oxygen desorption can result in the regeneration of active sites and thus enables the catalytic cycle of NO decomposition [21]. Lin et al. suggested that NO_2 species can be generated by the interaction between NO and oxygen atom over $YBa_2Cu_3O_7$ [25]. Over the 300 °C-reduced $La_{1.867}Th_{0.100}CuO_{4.005}$ sample, oxygen vacancies can stabilise O_2^- species and a high mobility of lattice oxygen favours the decomposition of $[O_2NO_2]^{2-}$. We envision that the redox action between O_2^- and O^{2-} is involved in the decomposition of NO.

4. Conclusion

When $La_{1.867}Th_{0.100}CuO_4$ was reduced at temperatures between 100 and 300 °C, it retained a single phase of K_2NiF_4-type structure, with oxygen vacancies and trapped electrons being created in the lattice. The K_2NiF_4-type structure collapsed at a reduction temperature of 500 °C to a mixture of oxides. After oxidation at 800 °C, the mixture was converted back to the former single phase. During the oxidation process, O_2^- species was generated at oxygen vacancies. The $La_{1.867}Th_{0.100}CuO_4$ sample reduced at 300 °C possessing cation defects and oxygen vacancies as well as Cu^+ ions exhibited better NO decomposition activity than the fresh and 100 °C-reduced samples. La_2CuO_4 showed relatively lower NO decomposition activity due to the absence of cation defects and oxygen vacancies in its lattice.

During NO adsorption, NO radicals and O_2^- were generated on both fresh and 300 °C-reduced samples, whereas $[O_2NO_2]^{2-}$ was only detected on the latter. We propose that $[O_2NO_2]^{2-}$ is a key intermediate for N_2 production. The redox between Cu^{2+} and Cu^+ as well as that between O_2^- and O^{2-} are involved in the decomposition of NO over the 300 °C-reduced catalyst.

Acknowledgement

The work described above was fully supported by a grant from the Hong Kong Baptist University (FRG/97-98/I-30).

References

[1] K. Tabata and M. Misono, Catal. Today 8 (1990) 249.
[2] Z.L. Yu, L.Z. Gao, S.Y. Yuan and Y. Wu, J. Chem. Soc. Faraday Trans. 88 (1992) 3245.
[3] S.D. Peter, E. Garbowski, N. Guilhaume, V. Perrichon and M. Primet, Catal. Lett. 54 (1998) 79.
[4] L.Z. Gao, Z.L. Yu and Y. Wu, in: *Proc. 34th IUPAC Congr.*, 1993, p. 730.
[5] L.Z. Gao, Z.L. Yu and Y. Wu, Acta Chim. Sinica 55 (1997) 56.
[6] M. Anpo, M. Matsuoka, Y. Shioya, H. Yamashita, E. Giamello, C. Morterra, M. Che, H.H. Paterson, S. Webber, S. Oullete and M.A. Fox, J. Phys. Chem. 98 (1994) 5744.
[7] E. Giamello, D. Murphy, G. Magacca, C. Morterra, Y. Shioya, T. Nomura and M. Anpo, J. Catal. 136 (1992) 510.
[8] J.W. London and A.T. Bell, J. Catal. 31 (1973) 96.
[9] N. Mizuno, M. Yamato and M. Tanaka, Chem. Mater. 1 (1989) 232.
[10] V.I. Pârvulescu, P. Grange and B. Delmon, Catal. Today 46 (1998) 233.
[11] G.J. Millar, A. Canning, G. Rose, B. Wood, L. Trewartha and I.D.R. Mackinnon, J. Catal. 183 (1999) 169.
[12] E.S.J. Lox and B.H. Engler, *Handbook of Heterogeneous Catalysis*, Vol. 4, eds. G. Ertl, H. Knözinger and J. Weitkamp (1997) p. 1628.
[13] L.K. Gushee and R. Ward, J. Am. Chem. Soc. 79 (1957) 5601.
[14] D.C. Harris and T.A. Hewton, J. Solid State Chem. 69 (1987) 182.
[15] C.T. Au and X.P. Zhou, J. Chem. Soc. Faraday Trans. 92 (1996) 1793.
[16] C. Morterra, E. Giamello, G. Gerrato, G. Centi and S. Perathoner, J. Catal. 179 (1989) 111.
[17] A. Martínez-Arias, J. Sorria, J.C. Conesa, X.L. Seoane, A. Arcoya, and R. Cataluña, J. Chem. Soc. Faraday Trans. 91 (1995) 1679.
[18] C. Oliva, L. Forni, A.M. Ezerets, I.E. Mukovozov and A.V. Vishniakov, J. Chem. Soc. Faraday Trans. 94 (1998) 587.
[19] Z.X. Zhang and K.J. Klabunde, Inorg. Chem. 31 (1992) 1706.
[20] Z. Zhao, X.G. Yang and Y. Wu, Sci. China B 28 (1998) 31.
[21] M. Iwamoto, H. Furukawa and S. Kagawa, in: *New Developments in Zeolite Science and Technology*, Stud. Surf. Sci. Catal., Vol. 28, eds. Y. Murakami, A. Iijima and J.W. Ward (Elsevier, Amsterdam, 1986) p. 943.
[22] Z. Sojka, M. Che and E. Giamello, J. Phys. Chem. B 101 (1997) 4831.
[23] H. Yasuda, T. Nitadori, N. Mizuno and M. Misono, Bull. Chem. Soc. Jpn. 66 (1993) 3492.
[24] F. Munakata, Y. Akimune, Y. Shichi, M. Akutsu, H. Yamaguchi and Y. Inoue, J. Chem. Soc. Chem. Commun. (1997) 63.
[25] J.Y. Lin, A.T.S. Wee, K.L. Tan, K.G. Neoh and W.K. Teo, Inorg. Chem. 32 (1993) 5322.
[26] H.X. Dai, C.F. Ng and C.T. Au, Catal. Lett. 57 (1999) 115.
[27] A. Gervasini, P. Carniti and V. Ragaini, Appl. Catal. B 22 (1999) 201.
[28] M. Iwamoto, H. Yahiro, K. Tanda, N. Mizuno, Y. Mine and S. Kagawa, J. Phys. Chem. 95 (1991) 3727.
[29] Z. Chajar, M. Primet and H. Praliaud, J. Catal. 180 (1998) 279.
[30] M. Shelf, Chem. Rev. 95 (1995) 209.
[31] Y.F. Chang and J.G. McCarty, J. Catal. 178 (1998) 408.
[32] J. Valyon and W.K. Hall, Catal. Lett. 19 (1993) 109.
[33] J. Valyon and W.K. Hall, J. Catal. 143 (1993) 520.
[34] J. Valyon, W.S. Millman and W.K. Hall, Catal. Lett. 24 (1994) 215.
[35] J. Sarkany, J.L. D'Itri and W.M.H. Sachtler, Catal. Lett. 16 (1992) 241.
[36] G.D. Lei, B.J. Adelman, J. Sarkany and W.M.H. Sachtler, Appl. Catal. B 5 (1995) 245.
[37] S.C. Larsen, A.W. Aylor, A.T. Bell and J.A. Reimer, J. Phys. Chem. 98 (1994) 11533.